

Sensor and Simulation Notes

Note 250

November 1977

Electromagnetic Wave Propagation Along a
Pair of Rectangular Bonded Wire Meshes

DAVID A. HILL

Institute for Telecommunication Sciences
National Telecommunications and Information Administration
U.S. Department of Commerce
Boulder, Colorado 80303

CLEARED
FOR PUBLIC RELEASE

PL/PA 5/15/97

Abstract-A mode equation is derived for propagation between a pair of rectangular wire meshes, and numerical results for the propagation constant of the quasi-TEM mode are presented. An approximate method based on averaged boundary conditions is found to agree if the mesh dimensions are small and the mesh separation is large. The field distribution of the quasi-TEM mode is also examined.

INTRODUCTION

The electromagnetic properties of wire mesh screens are of interest in numerous shielding and reflecting applications. The relevant plane wave scattering properties have been analyzed both for meshes in free space [1]-[4] and over a lossy earth [5]-[6]. The closely related problem of surface wave propagation on a wire mesh has also been analyzed [7]-[8].

In this paper, we consider propagation of electromagnetic waves between two parallel wire mesh screens. Such a configuration is used in electromagnetic pulse (EMP) parallel plate simulators [9]-[10] which are too large to employ solid metal sheets for the two conducting plates. Similar structures are also useful in cases where a slow-wave behavior is desirable [11]-[13].

DI 96-1128

ELECTROMAGNETIC WAVE PROPAGATION ALONG A
PAIR OF RECTANGULAR BONDED WIRE MESHES

ABSTRACT

A mode equation is derived for propagation between a pair of rectangular wire meshes, and numerical results for the propagation constant of the quasi-TEM mode are presented. An approximate method based on averaged boundary conditions is found to agree if the mesh dimensions are small and the mesh separation is large. The field distributed of the quasi-TEM mode is also examined.

electromagnetic wave propagation, TEM mode, wire meshes

INTRODUCTION

The electromagnetic properties of wire mesh screens are of interest in numerous shielding and reflecting applications. The relevant plane wave scattering properties have been analyzed both for meshes in free space [1]-[4] and over a lossy earth [5]-[6]. The closely related problem of surface wave propagation on a wire mesh has also been analyzed [7]-[8].

In this paper, we consider propagation of electromagnetic waves between two parallel wire mesh screens. Such a configuration is used in electromagnetic pulse (EMP) parallel plate simulators [9]-[10] which are too large to employ solid metal sheets for the two conducting plates. Similar structures are also useful in cases where a slow-wave behavior is desirable [11]-[13].

FORMULATION

The geometry of a single rectangular bonded mesh in free space (permittivity ϵ_0 and permeability μ_0) is illustrated in Fig. 1. Arrays of wires parallel to the x axis with spacing b and parallel to the y axis with spacing a are centered in the plane $z = 0$, and perfect contacts are made at the junctions. A second identical mesh is centered in the plane $z = -2d$ as illustrated in Fig. 2a. The wire radius c is small compared to the spacings a and b, the mesh separation 2d, and the free space wavelength λ . Consequently, only the axial wire currents are important and the usual thin wire approximations are valid.

Since the parallel plate mesh structure in Fig. 2a has a plane of symmetry at $z = -d$, the electromagnetic field can be decomposed into symmetric and antisymmetric parts which are uncoupled [14]. The rectangular components of the symmetric part of the electric field satisfy the following:

$$E_x(x,y,z) = E_x(x,y,-z-2d)$$

and

$$E_y(x,y,z) = E_y(x,y,-z-2d) \quad (1)$$

$$E_z(x,y,z) = -E_z(x,y,-z-2d)$$

For the symmetric part, it can be shown by image theory that the parallel mesh geometry of Fig. 2a is equivalent to the geometry in Fig. 2b where a perfect magnetic conductor is inserted at $z = -d$. Of course the equivalence is valid only for $z > -d$.

The rectangular components of the antisymmetric part of the electric field satisfy a similar relationship:

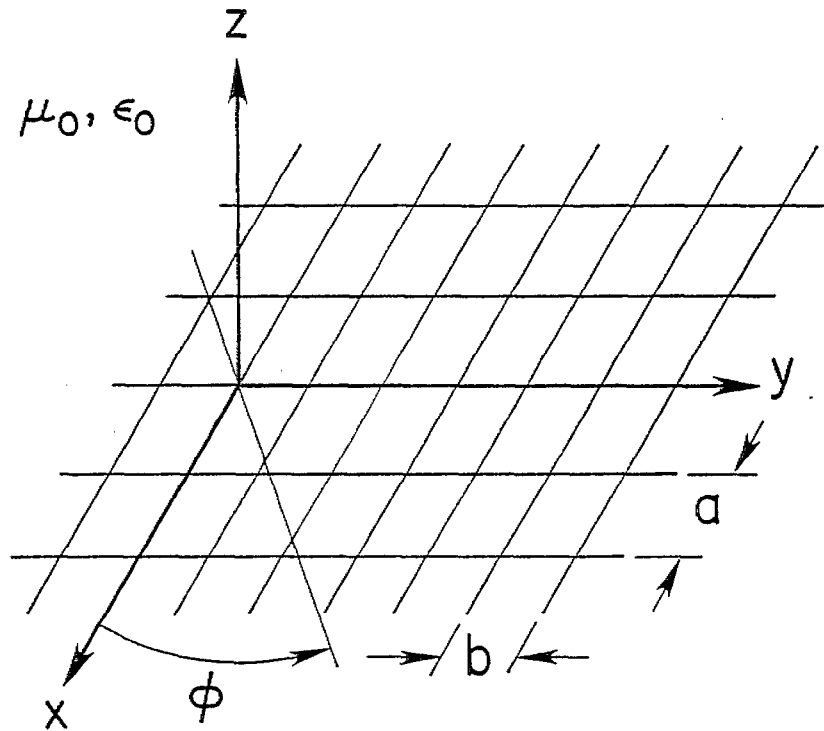


Figure 1. Geometry for a single rectangular wire mesh with bonded junctions. Wire radius equals c .

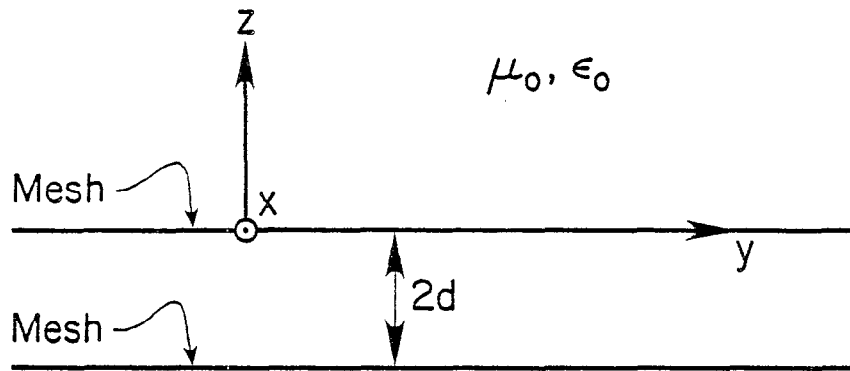


Figure 2a. A pair of identical meshes with separation $2d$.

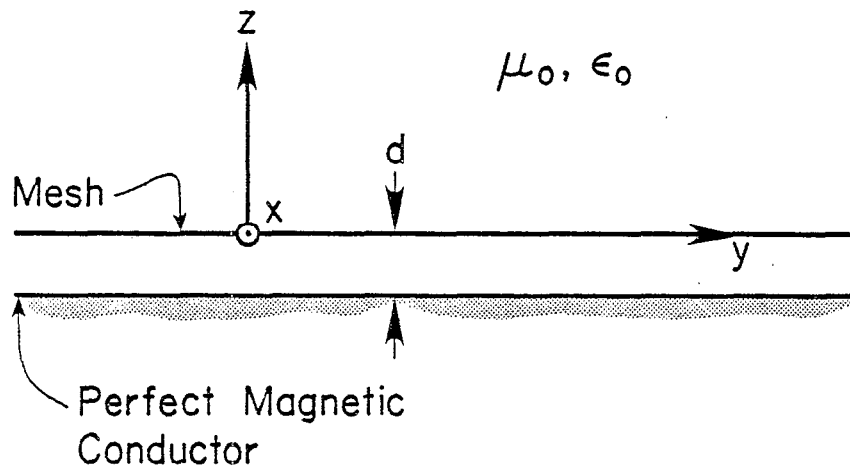


Figure 2b. Equivalent geometry for the symmetric part of the electromagnetic field.

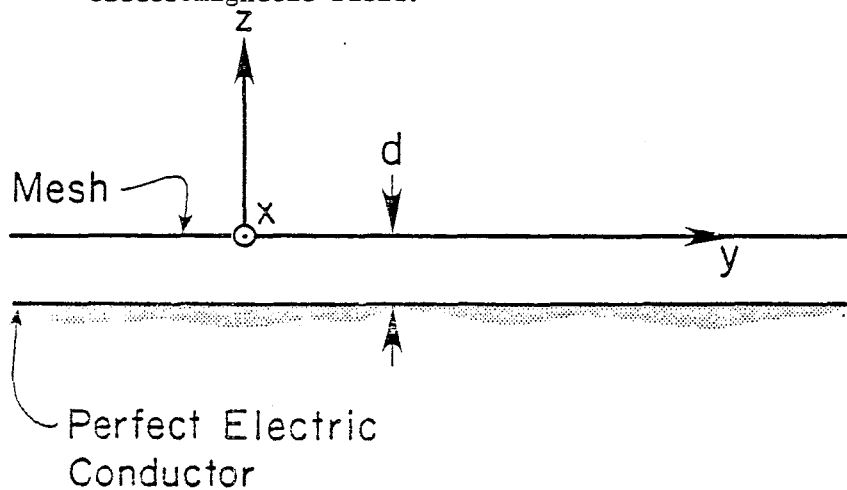


Figure 2c. Equivalent geometry for the antisymmetric part of the electromagnetic field.

$$\begin{aligned}
 & E_x(x,y,z) = -E_x(x,y,-z-2d) \\
 \text{and} \quad & E_y(x,y,z) = E_y(x,y,-z-2d)
 \end{aligned}
 \tag{2}$$

In this case, the parallel mesh geometry of Fig. 2a is equivalent (for $z > -d$) to the geometry in Fig. 2c where a perfect electric conductor is inserted at $z = -d$. This geometry will support a quasi-TEM mode which has no low frequency cutoff. Since this is the mode of primary interest in parallel plate simulators [9]-[10] and slow-wave structures [11]-[13], from here on we consider only the geometry in Fig. 2c.

The analysis closely follows that for a single rectangular bonded mesh in free space [8]. We seek modes which are propagating in x and y but which decay in z outside the guide ($z > 0$). We invoke Floquet's theorem [15] in order to express the relevant electromagnetic quantity as an exponential function multiplied by a function which is periodic in x and y . Thus for a single mode propagating at an angle ϕ to the negative x axis, the current on the q th x -directed wire I_{xq} and the current on the m th y -directed wire I_{ym} can be written:

$$I_{xq} = \exp[\gamma(x \cos\phi + qb \sin\phi)] \sum_m A_m \exp(i2\pi mx/a) \tag{3}$$

and

$$I_{ym} = \exp[\gamma(y \cos\phi + ma \sin\phi)] \sum_q B_q \exp(i2\pi qy/b) \tag{4}$$

A_m and B_q are the unknown Fourier coefficients, and γ is the propagation constant of the particular mode which we seek. The m and q summations are over all integers including zero from $-\infty$ to ∞ . The calculation of the fields produced by these currents in the presence of a perfectly conducting half-space is straightforward [6] and will not be

repeated here. The thin wire boundary condition for perfectly conducting wires is the following:

$$E_x(x, 0, c) = E_y(0, y, c) = 0 \quad (5)$$

Although (5) is only applied to the $m = 0$ and $q = 0$ wires, the periodic Floquet form of (3) and (4) assures that the boundary condition will be satisfied at all wires.

The expressions for the current in (3) and (4) are identical to those in the plane wave scattering case [6] except that γ has replaced ikS where k was the free space wave number ($=2\pi/\lambda$) and S was the sine of the incidence angle. Thus the previous equations for A_m and B_q [6] can be used with the following modifications: 1) set the incident fields equal to zero (source-free problem), 2) set the grid separation h equal to zero (bonded grids in the same plane), 3) set the wire impedances equal to zero (perfectly conducting wires), and 4) set the half-space conductivity equal to infinity. As a result, equations (24) and (26) in [6] reduce to the following:

$$A_m \frac{(k^2 - k_x^2) P_m}{2ikb} + \frac{ik_x}{2ka} \sum_q B_q k_y \left[\frac{\exp(-\Gamma c) - \exp(-2\Gamma d)}{\Gamma} \right] = 0, \quad (6)$$

$$B_q \frac{(k^2 - k_y^2) Q_q}{2ika} + \frac{ik_y}{2kb} \sum_m A_m k_x \left[\frac{\exp(-\Gamma c) - \exp(-2\Gamma d)}{\Gamma} \right] = 0, \quad (7)$$

where

$$P_m = \sum_q \left[\frac{\exp(-\Gamma c) - \exp(-2\Gamma d)}{\Gamma} \right], \quad (8)$$

$$Q_q = \sum_m \left[\frac{\exp(-\Gamma c) - \exp(-2\Gamma d)}{\Gamma} \right], \quad (9)$$

$$\Gamma_{mq} (= \Gamma) = (k_x^2 + k_y^2 - k^2)^{1/2}, \quad (10)$$

$$k_x = (2\pi m/a) + kS \cos\phi, \quad (11)$$

and

$$k_y = (2\pi q/b) + kS \sin\phi. \quad (12)$$

S is now defined as $\gamma/(ik)$. We note in passing that the case of symmetric modes (Fig. 2b) can be obtained from (6)-(9) by simply replacing the image term, $-\exp(-2\Gamma d)$, by $+\exp(-2\Gamma d)$ everywhere that it appears.

The summations involving $\exp(-\Gamma c)$ in (8) and (9) are rather slowly convergent as they stand. More rapidly convergent forms have been derived previously for P_m and Q_q in the free space case [8] and can be applied here to yield

$$P_m = \frac{b}{\pi} \left\{ -\ln \left[1 - \exp \left(\frac{-2\pi c}{b} \right) \right] + \Delta_m \right\} + \frac{\exp(-\Gamma_{mo} c)}{\Gamma_{mo}} - \sum_q \frac{\exp(-2\Gamma d)}{\Gamma}, \quad (13)$$

$$Q_q = \frac{a}{\pi} \left\{ -\ln \left[1 - \exp \left(\frac{-2\pi c}{b} \right) \right] + \delta_q \right\} + \frac{\exp(-\Gamma_{oq} c)}{\Gamma_{oq}} - \sum_m \frac{\exp(-2\Gamma d)}{\Gamma}, \quad (14)$$

where

$$\Delta_m = \frac{1}{2} \sum_q' \left[\frac{2\pi}{b} \frac{\exp(-\Gamma c)}{\Gamma} - \frac{\exp(-2\pi |q| c/b)}{|q|} \right] \quad (15)$$

and

$$\delta_q = \frac{1}{2} \sum_m' \left[\frac{2\pi}{a} \frac{\exp(-\Gamma c)}{\Gamma} - \frac{\exp(-2\pi |m| c/a)}{|m|} \right]. \quad (16)$$

The superscripted prime over the summation sign indicates omission of the $q = 0$ (or $m = 0$) term.

The doubly infinite set of linear equations (6) and (7) for A_m and B_q is numerically inefficient in the present form because A_m and B_q decay slowly for large $|m|$ and $|q|$. The difficulty arises because the current expansions in (3) and (4) are slowly convergent for the discontinuous current that occurs at the wire junctions in bonded meshes. We circumvent the convergence problem by modifying the current expansions to allow for a jump discontinuity at the origin. The procedure is nearly identical to that employed for the rectangular bonded mesh in free space [8] and a few of the details are omitted here. The Fourier coefficients of the current A_m and B_q are first rewritten [8]:

$$A_m = A'_m + \frac{\Delta(1-\delta_{m0})}{2\pi im} \quad (17)$$

and

$$B_q = B'_q - \frac{\Delta(1-\delta_{q0})}{2\pi iq} \quad (18)$$

where

$$\delta_{m0} = \begin{cases} 1, & m = 0 \\ 0, & m \neq 0 \end{cases}$$

A'_m and B'_q are modified current coefficients, and Δ is an unknown current discontinuity in I_{x0} at $x = 0$. By substituting (17) and (18) into (6) and (7), we obtain the following equivalent set of equations for the modified coefficients:

$$A'_m \frac{(k^2 - k_x^2) P_m}{2ikb} + \frac{ik_x}{2ka} \sum_q B'_q k_y \left[\frac{\exp(-\Gamma c) - \exp(-2\Gamma d)}{\Gamma} \right] \quad (19)$$

$$+ \Delta \left\{ \frac{(k^2 - k_x^2) P_m}{2kb} \frac{(\delta_{m0} - 1)}{2\pi m} - \frac{k_x}{2ka} \left[\frac{P'_m}{b} + \frac{kS \sin\phi}{2\pi} P_{1m} \right] \right\} = 0$$

and

$$\begin{aligned}
& B'_q \frac{(k^2 - k_y^2) Q_q}{2ika} + \frac{ik_y}{2kb} \sum_m A'_m k_x \left[\frac{\exp(-\Gamma c) - \exp(-2\Gamma d)}{\Gamma} \right] \\
& + \Delta \left\{ \frac{(k^2 - k_y^2) Q_q}{2ka} \frac{(1 - \delta_{q0})}{2\pi q} + \frac{k_y}{2kb} \left[\frac{Q'_q}{a} + \frac{kS \cos \phi}{2\pi} Q_{1q} \right] \right\} = 0
\end{aligned} \tag{20}$$

where

$$P'_{1m} = \sum_q \left[\frac{\exp(-\Gamma c) - \exp(-2\Gamma d)}{q\Gamma} \right], \tag{22}$$

$$P'_m = P_m - \left[\frac{\exp(-\Gamma_{mo} c) - \exp(-2\Gamma_{mo} d)}{\Gamma_{mo}} \right], \tag{22}$$

$$Q'_{1q} = \sum_m \left[\frac{\exp(-\Gamma c) - \exp(-2\Gamma d)}{m\Gamma} \right], \tag{23}$$

and

$$Q'_q = Q_q - \left[\frac{\exp(-\Gamma_{oq} c) - \exp(-2\Gamma_{oq} d)}{\Gamma_{oq}} \right] \tag{24}$$

Again the superscript prime ' on the summation indicates omission of the $q = 0$ (or $m = 0$) term. All summations are now in a rapidly convergent form.

Since we have introduced an additional unknown Δ , another equation is required to have an equal number of equations and unknowns (A'_m , B'_q , and Δ). The following equation can be obtained from charge continuity [8]:

$$\begin{aligned}
& -\frac{\Delta}{2\pi} \left(1 + \frac{b}{a} \right) + \sum_m A'_m \left(im \frac{b}{a} + \frac{ikSb}{2\pi} \cos \phi \right) \\
& - \sum_q B'_q \left(iq + \frac{ikSb}{2\pi} \sin \phi \right) = 0.
\end{aligned} \tag{25}$$

Since the doubly infinite set of equations, (19) and (20), are rapidly convergent, they can be truncated with m ranging from $-M$ to M and q ranging from $-Q$ to Q where M and Q are small integers. Thus (19),

the a/b ratio. For the cases considered here, convergence was obtained for $M = Q = 2$ ($T=11$) which is consistent with previous results [7]-[8]. All results shown here are for $M = Q = 2$, and the required determinant calculation is fairly rapid for the resultant 11×11 matrix. For comparison, some results from the method of averaged boundary conditions [12] have been calculated from (38).

In Fig. 3, we illustrate the ϕ dependence of S for various values of d/b . The a/b ratio of 3 was chosen because a 3 to 1 mesh has been used in some EMP simulators (private communication, C.E. Baum). In all results shown here, the c/b ratio is 10^{-2} , but the results are only weakly dependent on this ratio. Note that S always increases as ϕ goes from 0° to 90° . Because of symmetry, only the range of ϕ from 0° to 90° need be shown. As d/b is increased, the results approach a single mesh in free space ($d/b = \infty$). The dashed results obtained by the method of averaged boundary conditions are in rather poor agreement for $d/b = 1$. As the mesh spacing is increased, the agreement improves and is quite good for an isolated mesh ($d/b = \infty$). The reason for poor agreement for small d/b is probably that the effect of the higher order evanescent terms ($|m|$ and $|q| \neq 0$) is not accurately included in the method of averaged boundary conditions.

As discussed previously [7], the variation of S with frequency will result in dispersion when attempting to transmit a pulse. The frequency dependence of S for $\phi = 0^\circ$ is shown in Fig. 4 for $a/b = 1$. For this square mesh case ($a/b = 1$), the mesh has a nearly isotropic behavior and very little ϕ variation occurs. This is in agreement with an experimental study on a single square mesh by Ulrich and Tacke [16] and a quasi-static analysis by Andreasen and Tanner [17]. Note that the agreement with the method of averaged boundary conditions is again poor for

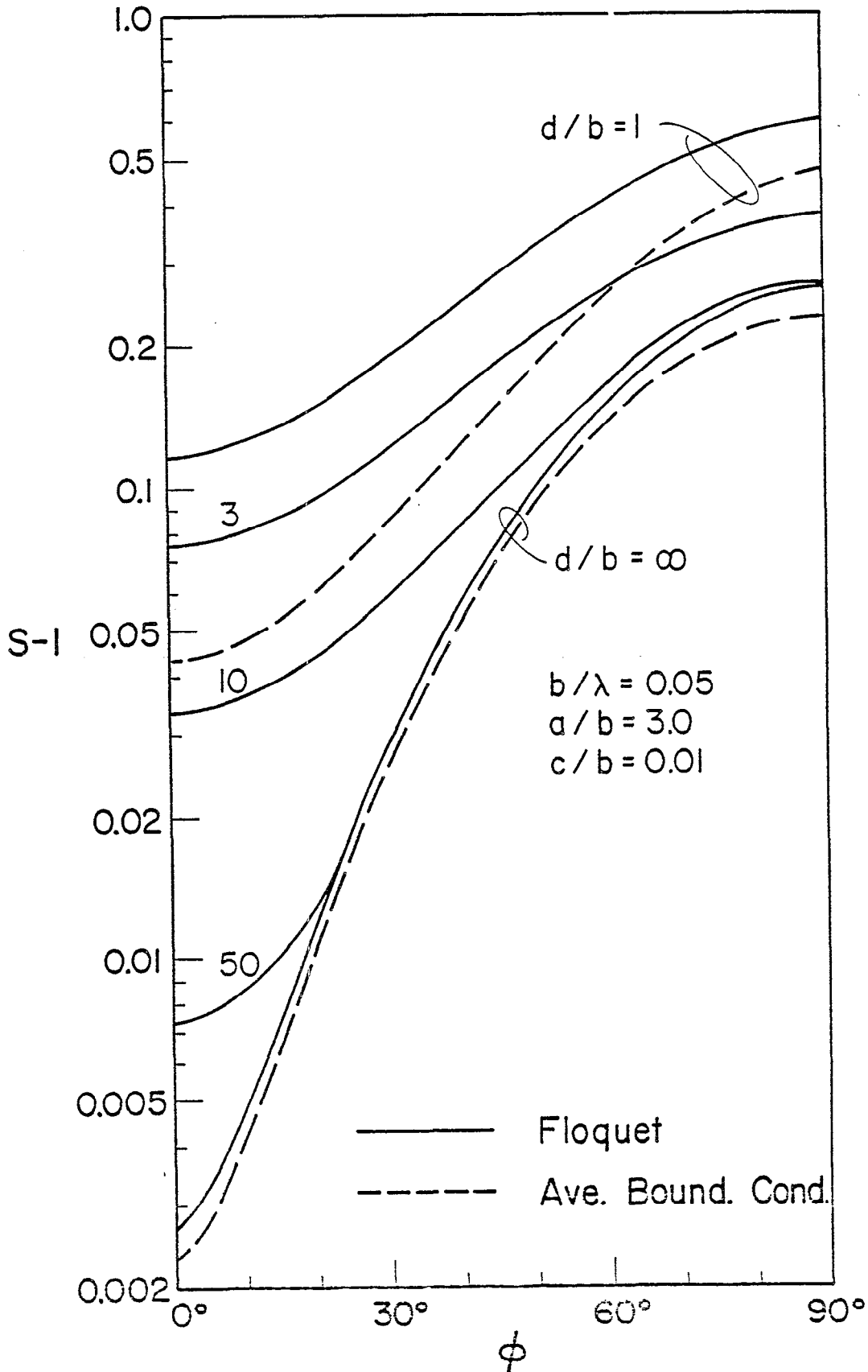


Figure 3. Normalized propagation constant S for a 3 to 1 mesh as a function of direction

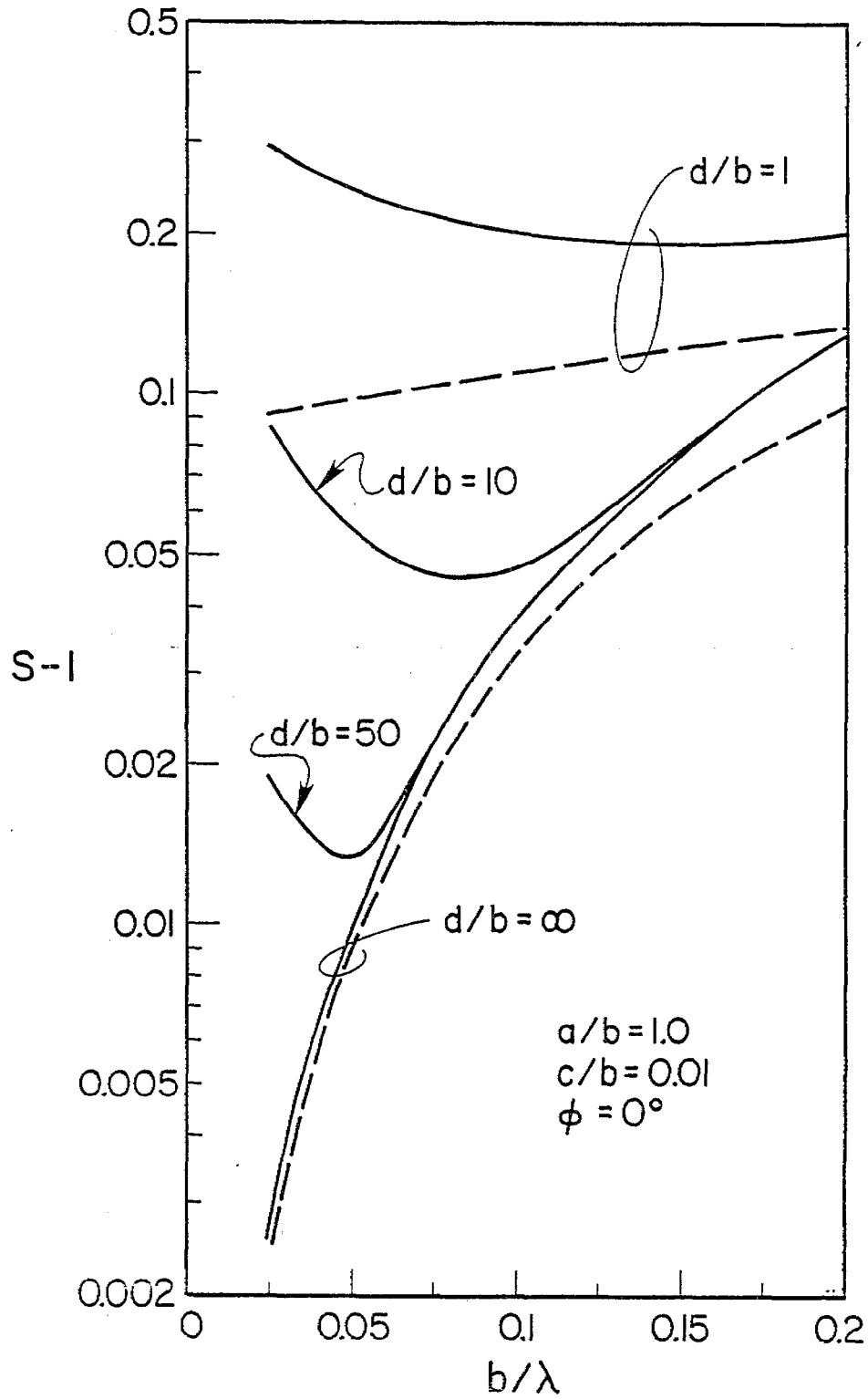


Figure 4. Frequency dependence of the propagation constant for propagation along the x-directed wires of a square mesh.

$d/b = 1$ and good for $d/b = \infty$. Also, both methods yield a value of S greater than one for b/λ approaching zero unless the mesh is completely isolated ($d/b = \infty$).

Similar results for a 3 to 1 mesh are shown in Fig. 5. The trends are similar but the values of S are smaller. This is due to the fact that there are fewer cross wires to contribute to the slow wave behavior of the guide. The effect of the cross wires has been described qualitatively as a periodic loading [16,17].

FIELD DISTRIBUTIONS

The field distribution inside a parallel mesh guide is of interest because a uniform plane wave field is desired in the working volume of EMP simulators. Also the field outside the meshes is important because of possible interference problems.

The fields of the currents given by (3) and (4) can be derived from an electric Hertz vector $\bar{\Pi}$ which has only x and y components [6]:

$$\bar{\Pi} = \hat{x}\Pi_x + \hat{y}\Pi_y, \quad (28)$$

where

$$\Pi_x = \frac{-i\eta_0}{2kb} \sum_m \sum_q A_m \left[\frac{\exp(-\Gamma|z|) - \exp(-\Gamma(z+2d))}{\Gamma} \right] \exp[i(k_x x + k_y y)] \quad (29)$$

$$\Pi_y = \frac{-i\eta_0}{2ka} \sum_m \sum_q B_q \left[\frac{\exp(-\Gamma|z|) - \exp(-\Gamma(z+2d))}{\Gamma} \right] \exp[i(k_x x + k_y y)], \quad (30)$$

$$\eta_0 = (\mu_0/\epsilon_0)^{1/2},$$

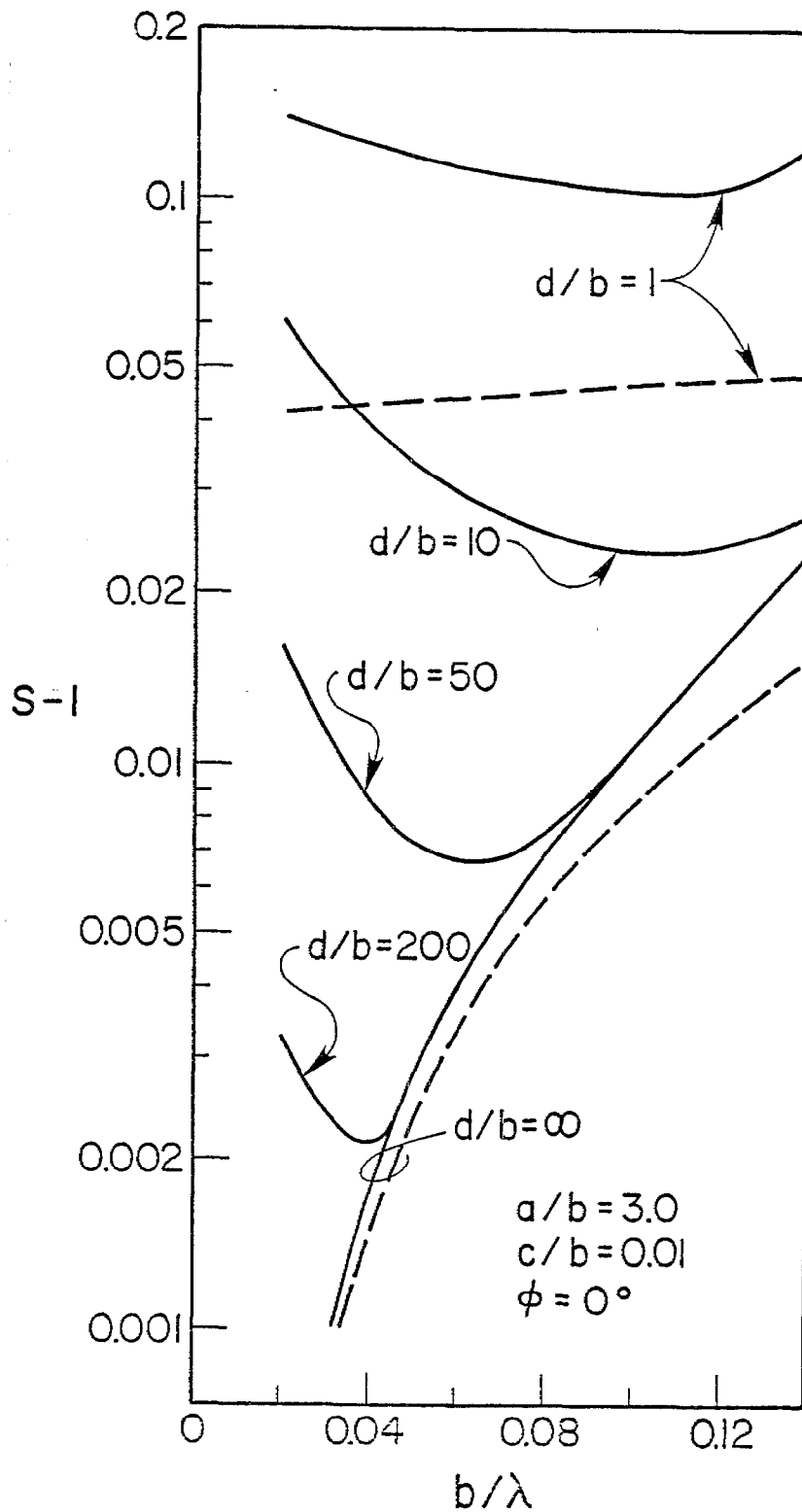


Figure 5. Frequency dependence of the propagation constant for propagation along the x-directed wires of a square mesh.

and \hat{x} and \hat{y} are unit vectors. Note that the fields for the symmetric modes (Fig. 2b) could be obtained by replacing the image term, $-\exp(-\Gamma(z+2d))$, by $+\exp(-\Gamma(z+2d))$ in (29) and (30). The electric and magnetic fields are obtained from the following operations on $\bar{\Pi}$:

$$\bar{E} = \nabla \nabla \cdot \bar{\Pi} + k^2 \bar{\Pi} \quad (31)$$

and

$$\bar{H} = \frac{ik}{\eta_0} \nabla \times \bar{\Pi} \quad (32)$$

In general, the expressions for \bar{E} and \bar{H} obtained by substituting (28)-(30) into (31) and (32) are rather complicated. However, for sufficiently small ka and kb only the constant terms ($m=q=0$) are of significance for observation points more than a cell dimension (a or b) from the mesh. An equivalent interpretation is that we consider the fields averaged over one cell, and only the $m = q = 0$ terms contribute. The constant terms for the Hertz components Π_{xo} and Π_{yo} are

$$\Pi_{xo} = \frac{-i\eta_0}{2kb} A_0 \left[\frac{\exp(-\Gamma_0 |z|) - \exp(-\Gamma_0 (z+d))}{\Gamma_0} \right] \exp \left[i(k_{ox}x + k_{oy}y) \right] \quad (33)$$

and

$$\Pi_{yo} = \frac{-i\eta_0}{2kb} B_0 \left[\frac{\exp(-\Gamma_0 |z|) - \exp(-\Gamma_0 (z+d))}{\Gamma_0} \right] \exp \left[i(k_{ox}x + k_{oy}y) \right] \quad (34)$$

where $k_{ox} = kS \cos\phi$, $k_{oy} = kS \sin\phi$, and $\Gamma_0 = k(S^2-1)^{1/2}$.

For general angle of propagation ϕ , all three components of the electric and magnetic fields can be non-zero. However, for the important special case of $\phi = 0^\circ$ (propagation along the x-directed wires) the fields simplify considerably because B_0 and k_{oy} are zero. Thus Π_{xo} and Π_{yo} simplify to

$$\Pi_{x0} = \frac{-i\eta_0}{2kb} A_0 \left[\frac{\exp(-\Gamma_0 |z|) - \exp(-\Gamma_0 (z + 2d))}{\Gamma_0} \right] \exp(ikSx) \quad (35)$$

and

$$\Pi_{y0} = 0.$$

Thus the constant components of the electric and magnetic fields are

$$H_{x0} = H_{z0} = E_{y0} = 0,$$

$$E_{x0} = \left(\frac{\partial^2}{\partial z^2} + k^2 \right) \Pi_{x0}, \quad E_{z0} = \frac{\partial^2 \Pi_{x0}}{\partial z \partial x}, \quad (36)$$

and

$$H_{y0} = \frac{ik}{\eta_0} \frac{\partial \Pi_{x0}}{\partial z}$$

By substituting (35) into (36), we obtain

$$E_{x0} = \frac{i\eta_0 A_0}{b} \exp(ikSx) E_{xon},$$

$$E_{z0} = \frac{\eta_0 A_0}{b} \exp(ikSx) E_{zon},$$

$$H_{y0} = \frac{A_0}{b} \exp(ikSx) H_{yon},$$

where

$$E_{xon} = (S^2 - 1)^{1/2} [\exp(-\Gamma_0 |z|) - \exp(\Gamma_0 (z + 2d))]/2, \quad (37)$$

$$E_{zon} = S[-\operatorname{sgn}(z)\exp(-\Gamma_0 |z|) + \exp(-\Gamma_0 (z + 2d))]/2,$$

$$H_{yon} = [-\operatorname{sgn}(z)\exp(-\Gamma_0 |z|) + \exp(-\Gamma_0 (z + 2d))]/2$$

and

$$\operatorname{sgn}(z) = \begin{cases} +1, & z > 0 \\ -1, & z < 0 \end{cases}.$$

Note that the normalized fields E_{xon} , E_{zon} , and H_{yon} are all real and dimensionless. This normalization implies that the mesh carries a fixed current density, A_0/b .

In Figs. 6-8, we illustrate the z dependence of E_{xon} , E_{zon} , and H_{yon} both inside ($z < 0$) and outside ($z > 0$) the guide for various values of S . Of course, in a specific example S is determined from the mode equation (27). Here we choose $d/\lambda = 1$, but it would be easy to generate results for other values of d/λ from (37). Note that for $S = 1$, we have essentially a perfect guide. All fields are zero outside the guide, and E_{zon} and H_{yon} are unity inside. E_{xon} is zero everywhere.

For the extremely slow wave case of $S = 2$, the fields are simply those of a slow surface wave on the mesh and decay rapidly on both sides of the mesh. For intermediate values of S , the values of the desired fields, E_{zon} and H_{yon} , decrease toward the center of the guide ($z = -d$) and are nonzero outside the guide. Also, E_{xon} becomes nonzero. This behavior is consistent with the known fact that the departure of S from unity is a measure of the shielding degradation for wire meshes [7], [8]. An important design consideration is that $2\Gamma_0 d (= 2k(S^2 - 1)^{1/2} d)$ must be kept small in order to produce a nearly constant field inside the guide and a small field outside the guide as desired in EMP simulators.

CONCLUDING REMARKS

A general formulation has been derived for the propagation modes of a pair of parallel rectangular meshes. The mode equation has been solved numerically for the propagation constant of the quasi-TEM mode. This is a slow-wave mode which has no low frequency cutoff, and it is the dominant mode in parallel mesh EMP simulators. For comparison, results from the method of averaged boundary conditions are also presented. The agreement

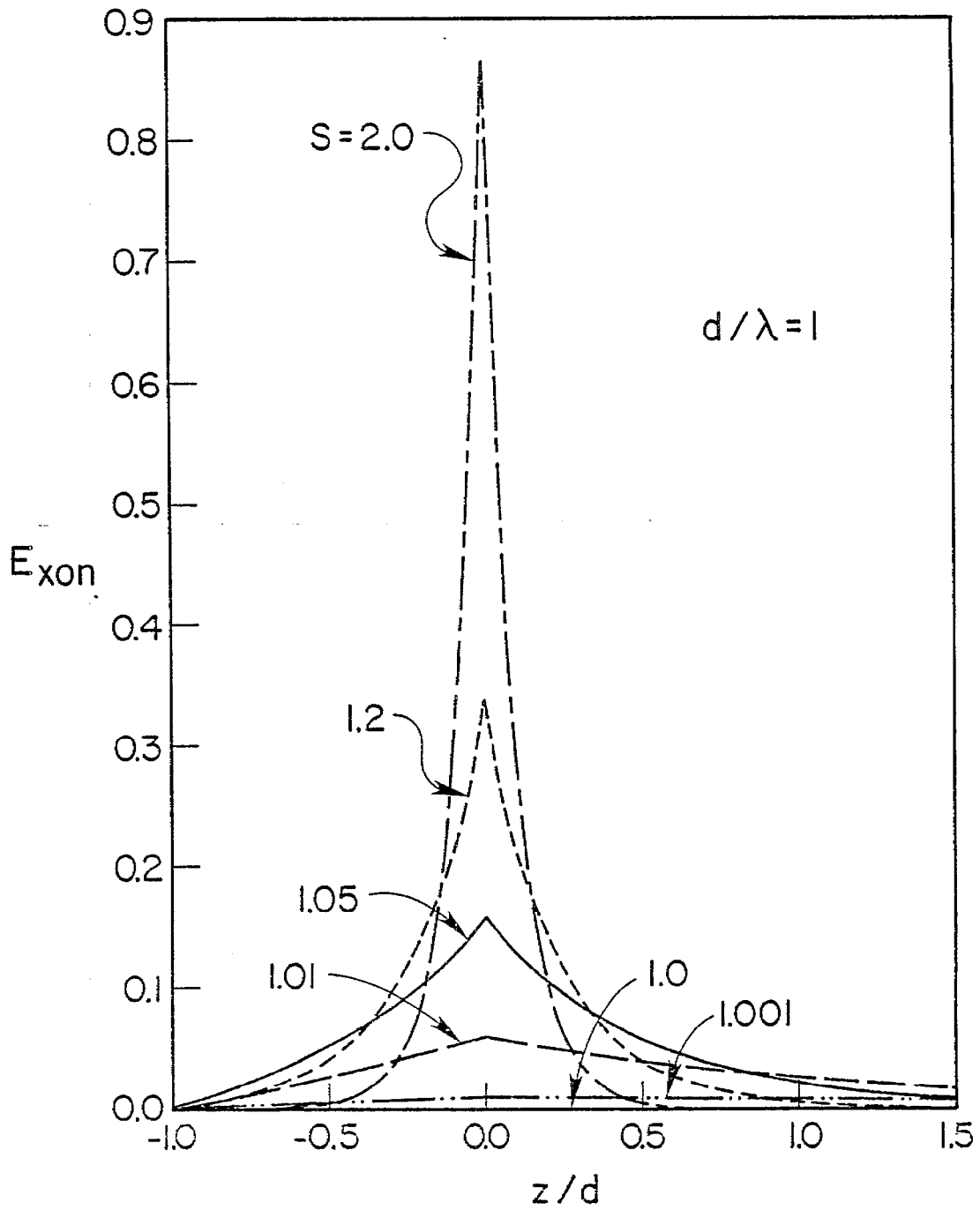


Figure 6. Distribution of the longitudinal electric field E_{xon} for various values of S .

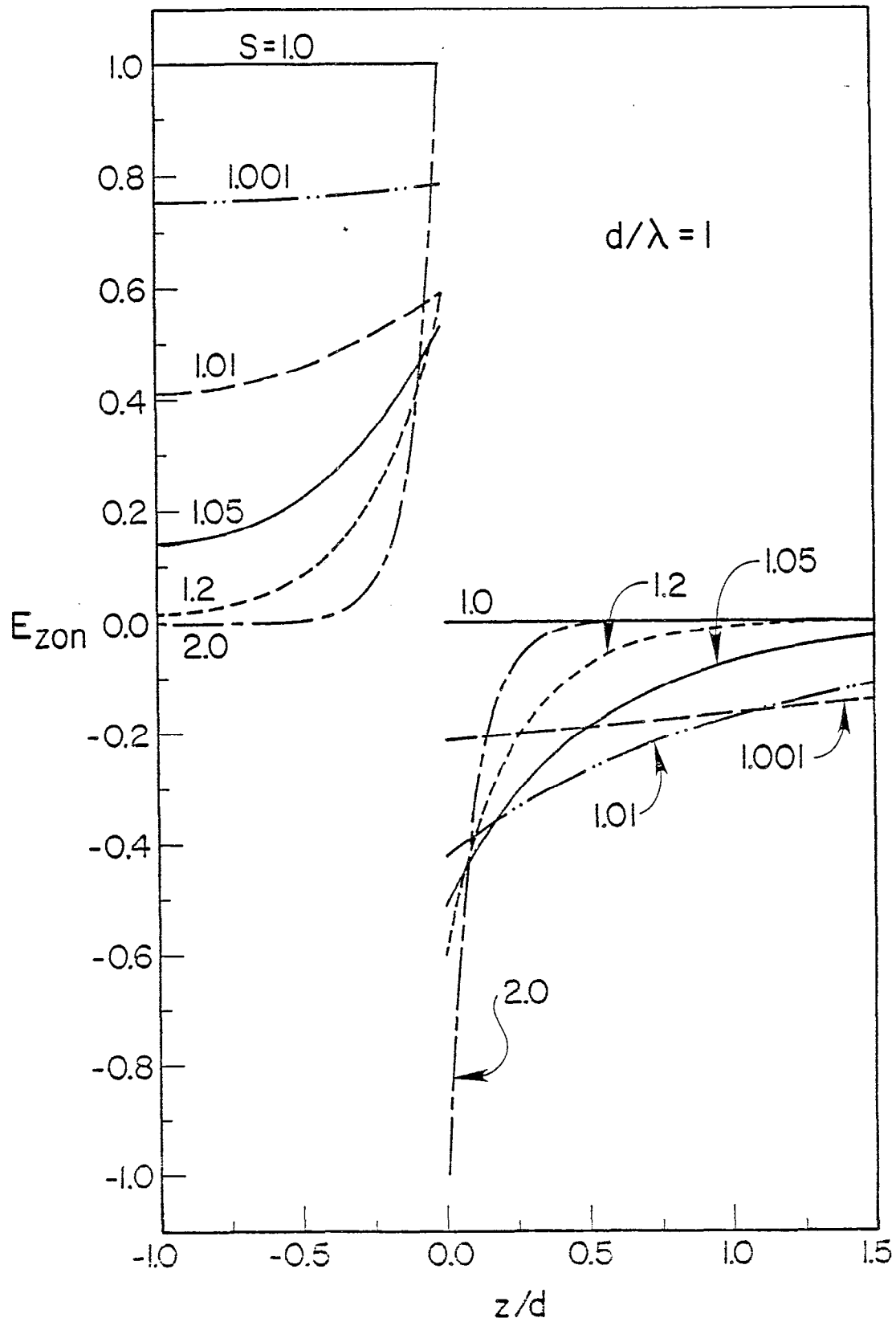


Figure 7. Distribution of the transverse electric field E_{zon} for various values of S .

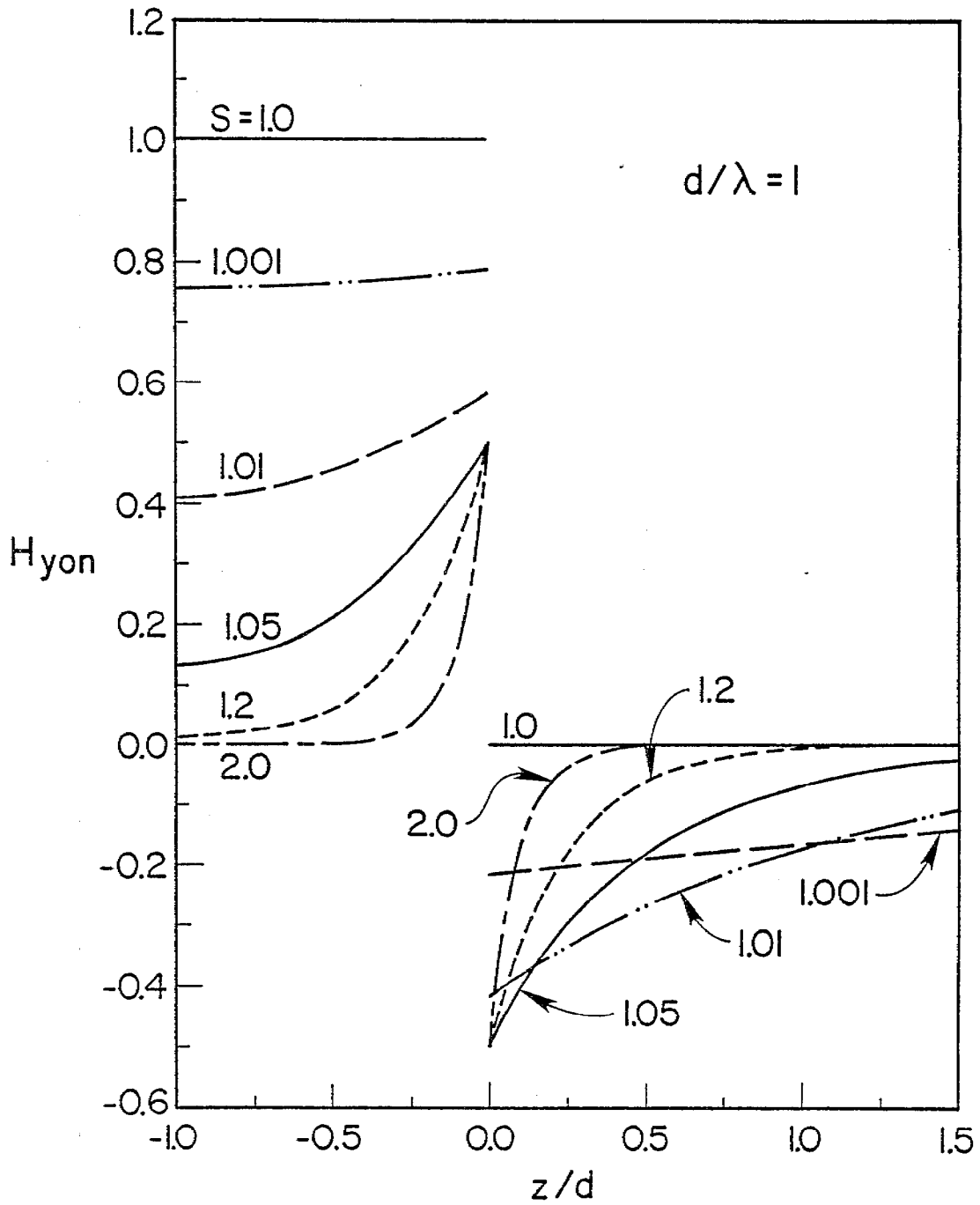


Figure 8. Distribution of the transverse electric field E_{zon} for various values of S .

between the two methods is good only when the mesh dimensions are small and the two meshes are widely separated. When the meshes are rectangular ($a \neq b$), the propagation constant is highly dependent on the propagation direction.

Field distributions are also shown for the quasi-TEM mode. When the propagation constant is equal to that of free space (perfect meshes), the interior fields are uniform and transverse, and the exterior fields are zero. As the propagation constant increases (as for realistic meshes), the interior fields decrease toward the center of the guide, and the exterior fields become nonzero.

Several extensions to this work are possible. Although the quasi-TEM mode is of most interest, higher order modes are possible and could be studied from the general mode equation (27) derived here. The introduction of a lossy half-space (rather than the perfect electric and magnetic conductors considered here) would be useful in modeling ground screens for antennas [5], [6]. In general, these extensions would result in complex propagation constants and a numerical search in the complex plane for solution of the mode equation. A final practical problem of interest is the effect of finite mesh width on the propagation constant and field distribution of the modes. Two possible approaches are to model the meshes as sheet impedances [8] or as a finite number of wires [18].

ACKNOWLEDGEMENT

The author would like to thank Drs. J.R. Wait and C.E. Baum for useful discussions on this problem and Mrs. L.R. Hope for help in preparing the manuscript.

APPENDIX - AVERAGED BOUNDARY CONDITIONS

The geometry of Fig. 2c has been treated by the method of averaged boundary conditions [12] which is based on small a/λ and b/λ . The resultant mode equation [12] can be written in the following form:

$$\begin{aligned} & \sin^2\phi\{(\Gamma_o/k)[1 - \exp(-2\Gamma_o d)] - X_2[1 - S^2(R_2 \sin^2\phi + R_1 \cos^2\phi)]\} \\ & \cdot \{[1 - \exp(-2\Gamma_o d)] + (\Gamma_o/k)X_1[1 - S^2(R_1 - R_2)\cos^2\phi]\} \\ & + \cos^2\phi\{(\Gamma_o/k)[1 - \exp(-2\Gamma_o d)] - X_1[1 - S^2(R_1 \cos^2\phi + R_2 \sin^2\phi)]\} \\ & \cdot \{[1 - \exp(-2\Gamma_o d)] + (\Gamma_o/k)X_2[1 - S^2(R_2 - R_1)\sin^2\phi]\} = 0 \quad (38) \end{aligned}$$

where

$$R_1 = \frac{a/b}{1 + a/b}, \quad R_2 = \frac{b/a}{1 + b/a},$$

$$X_1 = \frac{2b}{\lambda} \ln\left(\frac{b}{2\pi c}\right),$$

and

$$X_2 = \frac{2a}{\lambda} \ln\left(\frac{a}{2\pi c}\right).$$

This mode equation has been programmed and solved numerically for S by the bisection method [15].

For the important special case of $\phi = 0^\circ$, (38) simplifies to

$$(\Gamma_o/k)[1 - \exp(-2\Gamma_o d)] - X_1(1 - R_1 S^2) = 0. \quad (39)$$

In the limit of large d , the exponential term vanishes in (39) for $\text{Re}(\Gamma_o) > 0$, and we have:

$$(S^2 - 1)^{1/2} - X_1(1 - R_1 S^2) = 0. \quad (40)$$

This is precisely the mode equation for the rectangular mesh in free space which has an explicit solution for S [8].

The other limiting case of (39) is for small $\Gamma_0 d$. In this case, we can replace $\exp(-2\Gamma_0 d)$ by $1 - 2\Gamma_0 d$. With this approximation (39) can be solved explicitly for S :

$$S = \left[\frac{1 + 2kd/X_1}{R_1 + 2kd/X_1} \right]^{1/2} \quad (41)$$

Although the simplicity of (41) is attractive, we find that the method of averaged boundary conditions does not agree well with the rigorous Floquet analysis for closely spaced meshes (small d). This poor agreement is illustrated in Figs. 6-8. Consequently, the validity of (41) is questionable.

REFERENCES

- [1] M.I. Kontorovich, V. Yu. Petrunkin, N.A. Yesepekina, and M.I. Astrakhan, "The coefficient of reflection of a plane electromagnetic wave from a plane wire mesh", *Radio Engr. Elect. Phys.*, Vol. 7, pp. 222-231, 1962.
- [2] M.I. Astrakhan, "Reflecting and screening properties of plane wire grids", *Telecom. Radio Engr.*, Vol. 23, pp. 76-83, 1968.
- [3] D.A. Hill and J.R. Wait, "Electromagnetic scattering of an arbitrary plane wave by two nonintersecting perpendicular wire grids", *Can. J. Phys.*, Vol. 52, pp. 227-237, 1974.
- [4] D.A. Hill and J.R. Wait, "Electromagnetic scattering of an arbitrary plane wave by a wire mesh with bonded junctions", *Can. J. Phys.*, Vol. 54, pp. 354-361, 1976., and Section II of Sensor and Simulation Note 231, June 1977.
- [5] G.A. Otteni, "Plane wave reflection from a rectangular mesh ground screen", *IEEE Trans. Antennas Propagat.*, Vol. AP-21, pp. 843-851, 1973.
- [6] J.R. Wait and D.A. Hill, "Electromagnetic scattering by two perpendicular wire grids over a conducting half-space", *Radio Sci.*, Vol. 11, pp. 725-730, 1976., and Section IV of Sensor and Simulation Note 231, June 1977.
- [7] D.A. Hill and J.R. Wait, "Electromagnetic surface wave propagation over a bonded wire mesh", *IEEE Trans. Electromagn. Compat.*, Vol. EMC-19, pp. 2-7, 1977., and Section III of Sensor and Simulation Note 231, June 1977.
- [8] D.A. Hill and J.R. Wait, "Electromagnetic surface wave propagation over a rectangular bonded wire mesh", submitted to *IEEE Trans. Electromagn. Compat.*, and also Sensor and Simulation Note 249, October 1977.
- [9] C.E. Baum, "General principles for the design of Atlas I and II, Part I: Atlas: Electromagnetic design considerations for horizontal

- version", *Sensor and Simulation Note 143*, Air Force Weapons Laboratory, Jan. 1972.
- [10] L.W. Ricketts, J.E. Bridges, and J. Milletta, *EMP Radiation and Protective Techniques*. Appendix C, New York: John Wiley and Sons, 1976.
- [11] R.K. Arora, "Surface waves on a pair of unidirectional conducting screens", *IEEE Trans. Antennas Propagat.*, Vol. AP-14, pp. 795-798, 1966.
- [12] M.I. Kontorovich, M.I. Astrakhan, and M.N. Spirina, "Slowing down of electromagnetic waves by wire meshes", *Radio Engr. Elect. Phys.*, Vol. 9, pp. 1242-1245, 1964.
- [13] R.K. Arora, B. Bhat, and S. Aditya, "Guided waves on a flattened sheath helix", *IEEE Trans. Microwave Theory Tech.*, Vol. MTT-25, pp. 71-72, 1977.
- [14] C.E. Baum, "Interaction of electromagnetic fields with an object which has an electromagnetic symmetry plane", *Interaction Note 63*, Air Force Weapons Laboratory, March 1971.
- [15] R.W. Hamming, *Numerical Methods for Scientists and Engineers*. New York: McGraw-Hill, 1973, pp. 62-63.
- [16] R. Ulrich and M. Tacke, "Submillimeter waveguiding on periodic metal structure", *Appl. Phys. Lett.*, Vol. 22, pp. 251-253, 1973.
- [17] M.G. Andreasen and R.L. Tanner, "A wire-grid lens antenna of wide application Part II: Wave-propagating properties of a pair of wire grids with square, hexagonal or triangular mesh", *IRE Trans. Ant. Propagat.*, Vol. AP-10, pp. 416-439, 1962.
- [18] J.R. Wait, "Excitation of an ensemble of parallel cables by an external dipole over a layered ground", *AEU*, Vol. 31, pp. 489-493, 1977.